AJNR

MR Imaging and Localized Proton Spectroscopy of the Precentral Gyrus in Amyotrophic Lateral Sclerosis

Brian C. Bowen, Pradip M. Pattany, Walter G. Bradley, James B. Murdoch, Francisco Rotta, Akmal A. Younis, Robert C. Duncan and Robert M. Quencer

MR Imaging and Localized Proton Spectroscopy of the Precentral Gyrus in Amyotrophic Lateral Sclerosis

Brian C. Bowen, Pradip M. Pattany, Walter G. Bradley, James B. Murdoch, Francisco Rotta, Akmal A. Younis, Robert C. Duncan, and Robert M. Quencer

BACKGROUND AND PURPOSE: In the search for a diagnostic test for amyotrophic lateral sclerosis (ALS), especially upper motor neuron (UMN) involvement, MR imaging and proton spectroscopy techniques have each received attention, but their findings have not been correlated. The purpose of this study was to identify relationships among the results of current techniques, taking into account the severity of clinical UMN disease, so that objective measures of the pathogenesis of ALS may be established.

METHODS: Eighteen subjects with clinically diagnosed ALS and 12 healthy volunteers underwent MR imaging of the brain and localized proton MR spectroscopy. Water-suppressed spectra from the left precentral gyrus and from the left cuneus gyrus were analyzed with the LCModel method, yielding concentrations for *N*-acetyl (NA), total creatine (Cr), choline (Cho), glutamate (Glu), glutamine (Gln), and *myo*-inositol (Ins) metabolic substrates. Signal intensities of the precentral gyrus on T2-weighted images were assessed qualitatively in a blinded fashion.

RESULTS: For the precentral gyrus, mean Cho (1.3 mM) and Ins (3.25 mM) for the ALS group were significantly increased. After adjustment for Cr covariance, mean Glu (5.08 mM) and NA (6.31 mM) were decreased. For the cuneus gyrus, no difference in metabolite concentrations between groups was observed. Trend analysis of the precentral gyrus metabolite concentrations revealed significant increases in Cho and Ins and decreases in NA and Glu with respect to the severity of clinical UMN signs. Metabolic changes were greater in the subset of ALS patients with precentral gyrus signal changes on imaging, and significantly increased Ins was associated with cortical hypointensity on fast spin-echo images.

CONCLUSION: Mean metabolite concentrations determined from precentral gyrus spectra reflect clinical and pathologic changes that occur in ALS. Imaging findings, while related to the spectral and clinical results, are not specific to ALS.

Amyotrophic lateral sclerosis (ALS), or motor neuron disease (MND), is a neurodegenerative disorder of unknown origin, occurring in sporadic (90–95% of cases) and familial (5–10%) forms (1). It is characterized pathologically by selective degeneration of somatic motor neurons of the brain stem and spinal cord (lower motor neurons) and large pyramidal neurons of the motor cortex (upper motor neurons [UMNs]), with eventual loss of fibers in the corticospinal tracts (CST) (2). Currently, the an-

temortem diagnosis of sporadic ALS is based on a spectrum of clinical, electrophysiological, and, sometimes, muscle biopsy findings (3). There is no definitive diagnostic test for the disease, and there is no established technique for demonstrating UMN involvement except for the clinical neurologic examination. For these reasons, there has been an interest in the last decade in the diagnostic value of in vivo MR imaging and spectroscopy of the brain in patients with suspected ALS.

MR imaging studies using T2-weighted and proton density–weighted spin-echo (4–6) or fast spin-echo (FSE) sequences (7) have shown that qualitatively increased signal intensity in the CST or decreased signal intensity in the precentral gyrus gray matter (motor cortex) or both occur in some patients with ALS. To our knowledge, no attempt has been made to relate the signal change in the precentral gyrus to clinical disease severity or to objective in vivo measures of precentral gyrus metabolism in these patients. Moreover, we know of no study in which the signal characteristics of the

precentral gyrus have been assessed in ALS patients by using fluid-attenuated inversion-recovery (FLAIR) imaging, which is highly sensitive for detecting cortical and subcortical lesions (8).

In vivo proton spectroscopy studies of the precentral gyrus (motor cortex) region in ALS patients have shown one of the following: a decrease in the peak area ratio of *N*-acetyl aspartate to total creatine (NAA/Cr) (9–11), in the ratio of NAA to Cr plus choline (NAA/[Cr + Cho]) (12), or in the absolute concentration of NAA (13). Because NAA is considered a neuronal marker, these results have been interpreted as evidence of UMN degeneration, consistent with pathologic findings (14). Most of the studies have used a point-resolved spectroscopy (PRESS) pulse sequence with long-TE values ($\geq$135). Thus, little has been published regarding metabolites, such as *myo*-inositol (Ins), glutamate (Glu), and glutamine (Gln), that have relatively short T2 relaxation times and J-coupled resonances. The latter two are of interest because recent laboratory evidence suggests that Glu excitotoxicity plays a significant role, as does free radical–mediated oxidative injury, in the progressive degeneration and ultimate death of motor neurons in ALS (15–17). Short-TE PRESS or stimulated-echo acquisition mode (STEAM) spectra (11) allow improved detection of Glu and Gln signals, yet determination of the relative concentrations of these metabolites at 1.5 to 2.0 T using standard spectral analysis programs (18, 19) is limited because of overlap of the coupled resonances. An alternative method of spectral analysis, the LCModel (20), has been used to obtain absolute concentrations of cerebral metabolites in clinically normal individuals from short-TE STEAM spectra (21, 22). In a preliminary study, this method has also been applied to short-TE PRESS spectra acquired from the brain stem in ALS patients (23).

The purpose of this study of the precentral gyrus was to determine how the results of current MR imaging (FSE, FLAIR) and single-voxel spectroscopy (short-TE STEAM) techniques relate to each other and to the degree of UMN degeneration in ALS subjects, as assessed clinically. The goals were to identify which measurements may be useful for the diagnosis and treatment of ALS and whether the results are consistent with proposed mechanisms for the pathogenesis of ALS.

Methods

Patients

Eighteen patients (six women and 12 men; age range, 26–71 years, mean $\pm$ SD, 54 $\pm$ 13 years), with probable (seven patients) or definite (11 patients) ALS on the basis of El Escorial criteria (3), were referred for MR imaging/spectroscopy. The interval between onset of symptoms and MR evaluation was 18 $\pm$ 15 months (mean $\pm$ SD; range, 2–56 months). At the time of the MR study, the severity of UMN abnormality in the face/neck and upper limb was graded as mild, moderate, or severe by two experienced neurologists. Four patients were taking no medications. Fourteen patients, who were being treated with either gabapentin or riluzole, had their medication discontinued for 2 weeks prior to the initial MR study and then reinstituted immediately afterward. Of these 14 patients, eight returned for a second MR study and clinical neurologic examination while on medication. For five of the patients (serial subgroup A), the time between the first and second MR studies was 2 weeks. For the remaining three patients (serial subgroup B), the intervals were 4 weeks, 10 weeks, or 18 weeks. As a control group, 12 healthy volunteers (eight women and four men; age range, 41–78 years; mean age $\pm$ SD, 59 $\pm$ 12 years) underwent the same MR study.

MR Imaging

The MR study was performed on a 1.5-T clinical scanner and consisted of an initial imaging component followed by proton spectroscopy. Axial T1-weighted spin-echo images (650/20/1 [TR/TE/excitations]), proton density–weighted and T2-weighted FSE images (3555/16,96$_{eff}$/1), and fast FLAIR images (7155/112/1, TI = 2000) were obtained with the same slice thickness (5 mm), gap (1 mm), field of view (FOV) (230 mm), and matrix (256 $\times$ 256). For the purpose of voxel placement, additional coronal and parasagittal T1-weighted, spin-echo pilot images (200/20/1) with a thickness of 5 mm, no gap, an FOV of 300, and a matrix of 128 $\times$ 256 were acquired. Visual interpretation of images of ALS and control subjects was done independently by two experienced neuroradiologists without knowledge of the neurologic diagnosis or clinical findings. The signal intensity of cortical gray matter (motor cortex) and that of the subcortical white matter in the precentral gyri on the T2-weighted FSE and FLAIR supraventricular axial images were compared visually with similar gray and white matter regions in the middle frontal and postcentral gyri. Hypointense signal in the gray matter or hyperintense signal in the white matter was considered definitely present when seen on two or more axial images. In cases in which there was disagreement between the two interpreters, a second review of the images was done jointly and a consensus was reached.

MR Spectroscopy

In all 30 subjects, localized proton spectra were acquired from an 8-mL voxel (2 $\times$ 2 $\times$ 2 cm) encompassing the left precentral gyrus superiorly (Fig 1A). In 18 of the subjects (11 ALS patients and seven volunteers), spectra were also acquired from the left cuneus gyrus in the occipital lobe (Fig 1B). In the remaining 12 subjects (seven ALS patients and five volunteers), spectra were acquired from the brain stem rather than the occipital lobe; however, these results will be presented as part of a future study.

Identification of the precentral gyrus, based on anatomic landmarks (24), and voxel placement were done by one neuroradiologist. The precentral gyrus location was verified by the second neuroradiologist during the above-described image interpretation session. Segmentation of the voxel contents into brain and CSF fractions on axial T1-weighted images was done manually and off-line on an imaging workstation using an interactive, mouse-driven program. This procedure used custom-designed software that displayed the voxel borders, which were orthogonal to the imaging plane, on all axial images intersected by the voxel.

Water-suppressed spectra were acquired using a STEAM pulse sequence (1500/20, mixing time = 13), with 256 accumulations, a bandwidth of $\pm$ 1000 Hz, and 2048 data points. Spectroscopic time-domain data were corrected for residual eddy current effects (25). To account for subject-to-subject variability in coil loading, the unsuppressed water signal for each subject was divided by the mean of the unsuppressed water signal for all subjects (patients plus controls), and this ratio was multiplied by the concentration results for that sub-
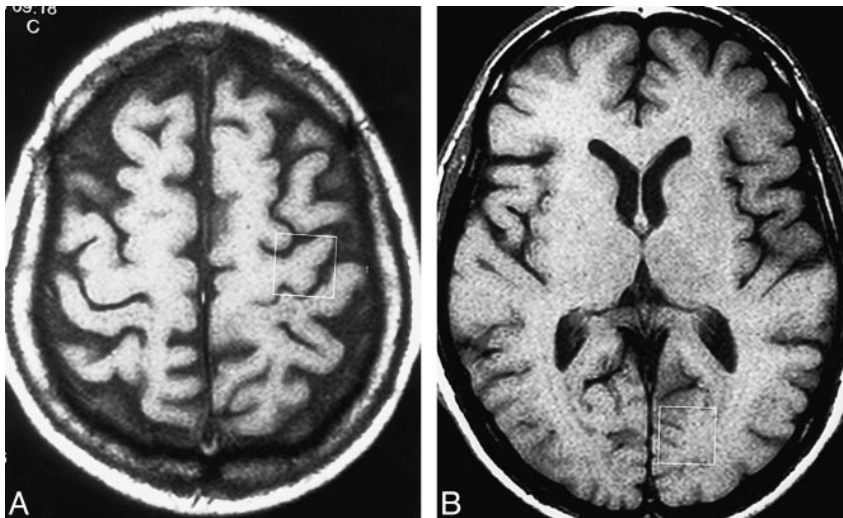
Fig 1. Voxel location in a 60-year-old man with definite ALS and clinically severe UMN signs.
  A, Precentral gyrus.
  B, Cuneus gyrus.

ject. Spectral analysis was performed using the LCModel (20), a user-independent, time-domain fitting routine that employs a basis set of concentration-calibrated model spectra of individual metabolites to estimate the absolute concentrations of similar brain metabolites from the in vivo spectral data. This method exploits the full spectroscopic information of each metabolite and not just isolated resonances (Fig 2). By applying the complete spectra rather than individual peaks, the information in complex spectra is fully used and can permit separation of metabolites, even when there are some overlapping peaks. Glycerophosphorylcholine (GPC) is included in the library of model spectra, as has been recommended by other investigators (22). The concentration of in vivo Cho is expressed as the sum of phosphorylcholine (PCh) and GPC (20–22). Because *N*-acetylaspartylglutamate (NAAG) is co-localized with NAA in neurons (26), the combined concentration of the two metabolites is reported in this study and is referred to as NA. Also reported are those metabolite concentrations that can be determined reliably with the LCModel (22): Cr + phosphocreatine, Ins, Glu, Gln, and Glu + Gln (Glx).

In two ALS patients, who had only an initial MR study, a poor fit of the precentral gyrus spectral data was obtained, yielding a Gln concentration equal to zero. These two spectra were omitted from the statistical analysis of the initial MR study data, which therefore assessed the results of 16 ALS and 12 control spectra from the precentral gyrus, and 11 ALS and seven control spectra from the cuneus gyrus. In one of the 16 ALS patients, the FLAIR and T2-weighted FSE images were degraded by patient motion, and in one of the control subjects, no FLAIR images were obtained. Thus, statistical tests of the relationship between precentral gyrus imaging findings and metabolite data were applied to 15 of the 18 ALS patients and 11 of the 12 control subjects.

Statistical Methods

Initial comparisons between the ALS and control spectral results (initial MR study) were done for age, voxel brain fraction (precentral gyrus), and metabolite concentrations by using a two-sided unpaired *t*-test. Following correlational analyses, which showed that some metabolites were correlated with Cr levels, we performed an analysis of covariance (ANCOVA) for each metabolite, using Cr as the covariate. This has the effect of adjusting metabolite levels for differences in Cr levels. An analysis of variance (ANOVA) was used to test for differences among metabolite concentrations as a function of clinical severity (control, mild, moderate, severe) and among groups categorized as to the likelihood of disease (control, probable ALS, definite ALS). These analyses were followed by trend analyses

using simple linear regression. To control the experimental error rate, we performed multiple comparisons and trend analyses between clinical severity groups and likelihood of disease groups only if the ANOVA and ANCOVA among groups was statistically significant ($P < .05$). The spectral results for ALS patients with and without signal changes in the precentral gyrus on FSE and FLAIR images were also compared as previously described. Among ALS patients who had two visits, paired *t*-tests were used to compare spectral results between the first and second visits.

Results

MR Spectroscopy

Representative spectra from the left precentral gyrus and the left cuneus gyrus of a patient with clinically severe ALS are shown in Figures 2A and B, respectively. The metabolic concentrations that were calculated from the STEAM spectral data for the initial MR study are presented in Table 1. For the precentral gyrus, there was no significant difference in the mean fraction of brain tissue within the voxel for the ALS group as compared with the control group. The LCModel concentrations shown in the Table have not been corrected for the brain partial volume result. The mean metabolite concentrations of the ALS group in the precentral gyrus differed from those of the control group by -6% for NA, $+13\%$ for Cho, -13% for Glu, -14% for Gln, and $+24\%$ for Ins (Table 1). Only the Cho and Ins results were significant by the two-sided unpaired *t*-test. No differences were observed for any of the metabolites in the cuneus gyrus.

Correlation analysis of the precentral gyrus metabolite concentrations, as well as of subjects' ages, for the combined groups (28 subjects) revealed a correlation between Cr and NA (pooled Pearson correlation coefficient $r = .50$, and $P = .006$) and between Cr and Glu ($r = .44$, $P = .018$). There was no correlation between age and any of the metabolite concentrations. A similar analysis of the cuneus gyrus concentrations revealed no correlations.
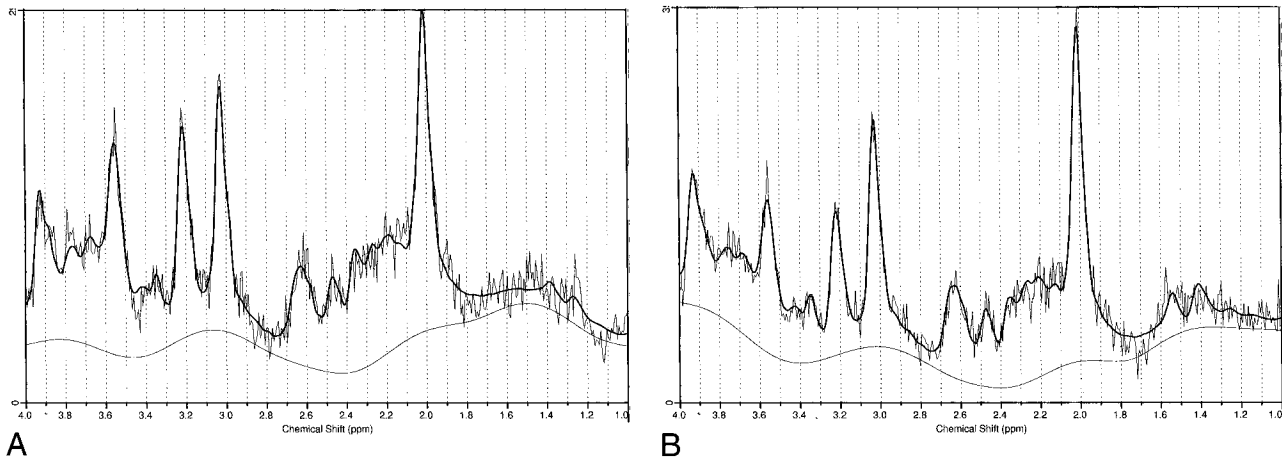
FIG 2.   Proton spectra from same subject and voxel locations as shown in Figure 1. The *dark line* represents the LCModel fit of the spectrum. The assignments of the principal peaks (in ppm) in the in vivo spectrum are as follows: NA = NAA (2.01) + NAAG (2.05), Cr (3.03), Ins (3.56). The complex multiplets of Glu and Gln, whose sum is Glx, are located at approximately 2.1 to 2.5 ppm and 3.7 to 3.8 ppm (see [41]).
A, Precentral gyrus.
B, Cuneus gyrus.

Regression analysis of the precentral gyrus metabolite concentrations for the ALS group and for the control group separately showed a linear relation between NA and Cr, which was similar in each group (Fig 3A). A linear relation between Glu and Cr, which was similar for the two groups, was also found (Fig 3B). By analysis of covariance, with NA and Glu each adjusted for the Cr relationships, the difference in precentral gyrus NA between the ALS and control groups approached significance ($P = .059$) and the difference in Glu reached significance ($P = .048$) (Table 1). Regression analysis of the cuneus gyrus data showed no relationships among metabolite concentrations.

Based on the clinical neurologic examination at the time of the initial MR study, six of the 16 patients with precentral gyrus spectral data had a diagnosis of probable ALS, while the remainder had a diagnosis of definite ALS. No significant differences in metabolite concentrations between these two ALS subgroups were found. The severity of clinical findings attributable to UMN disease was rated as mild in six patients, moderate in six, and severe in four. Figure 4 presents the histograms of mean concentration of NA, Cho, Glu, and Ins in the precentral gyrus for control subjects and ALS clinical severity subgroups. By analysis of covariance, with adjustment for Cr, there was a significant difference ($P = .044$) in NA values when classified by clinical severity. In pairwise *t*-tests following the analysis of covariance, patients with moderate or severe UMN deficits had significantly lower NA values ($P < .05$) as compared with control subjects, and there was a significant negative linear trend in values overall ($P = .005$) (Fig 4A). Ins values also differed significantly ($P = .01$) when classified by clinical severity. They were significantly higher ($P < .05$) in patients with moderate or severe deficits, and showed a highly significant positive linear

trend ($P = .001$) (Fig 4D). For Cho values, pairwise *t*-tests revealed that only patients with severe clinical UMN deficits had significantly higher ($P < .05$) Cho concentrations than control subjects. There was a significant positive linear trend ($P = .022$) in Cho values overall (Fig 4B). Although mean Glu values for each clinical severity subgroup were not significantly different, the negative trend relative to control subjects approached significance ($P = .094$) (Fig 4C). The remaining metabolites that were assessed (Glx, Gln, and Cr) showed no significant differences among the clinical severity subgroups and no significant trend in overall values.

The difference in metabolite concentrations between the initial MR study and a second study for serial subgroups A and B of ALS patients is presented in Table 2. For serial subgroup A, the interval between the first and second visits was 2 weeks, and no significant difference in metabolite concentrations was observed. For serial subgroup B, the mean interval was 11 weeks, and a significant decrease ($P = .022$) in NA was found. Clinically, there was no improvement in the severity of UMN signs between the first and second visits.

MR Imaging

The signal intensity of cortical gray matter and subcortical white matter in both precentral gyri were compared visually with corresponding regions in the middle frontal and postcentral gyri for T2-weighted FSE and FLAIR images (Fig 5). As shown in Table 3, for the FSE images, the observers agreed on the assessment of gray matter in 87% of patients and agreed on the assessment of white matter in 93% of patients. For the FLAIR images, the agreement was 100% for gray matter and 87% for white matter. The consensus results of the two

TABLE 1: Metabolite concentrations (mean ± SEM, mmol/L) from STEAM (TE = 20) spectra

Location	Group	No. of Subjects	Age	NA	Cho	Cr	Glu	Gln	Ins	Voxel*
Precentral	ALS	16	55 ± 3	6.31 ± 0.15	1.3 ± 0.04	5.74 ± 0.18	5.08 ± 0.23	3.66 ± 0.23	3.25 ± 0.09	0.87 ± 0.01
	Control	12	59 ± 3	6.74 ± 0.2	1.15 ± 0.04	5.77 ± 0.19	5.82 ± 0.32	4.28 ± 0.31	2.63 + 0.18	0.86 ± 0.01
	P		NS‡	.088	.023	NS	.065	NS	.003	NS
	P(adj Cr)†		NC‡	.059	NC	NC	.048	NC	NC	NC
Cuneus	ALS	11	50 ± 4	7.39 ± 0.19	1.03 ± 0.06	6.56 ± 0.23	6.39 ± 0.35	4.27 ± 0.52	3.2 ± 0.12	
	Control	7	58 ± 5	7.57 ± 0.24	1.13 ± 0.11	6.87 ± 0.2	7.22 ± 0.8	4.75 ± 0.65	3.18 ± 0.1	
	P		NS	NS	NS	NS	NS	NS	NS	

Note.—NA, N-acetyl (NAA + NAAG); Cho, choline; Cr, total creatine; Glu, glutamate; Gln, glutamine; Ins, myo-inositol.
* Fraction of voxel occupied by brain tissue.
† P value after adjusting for creatine covariance.
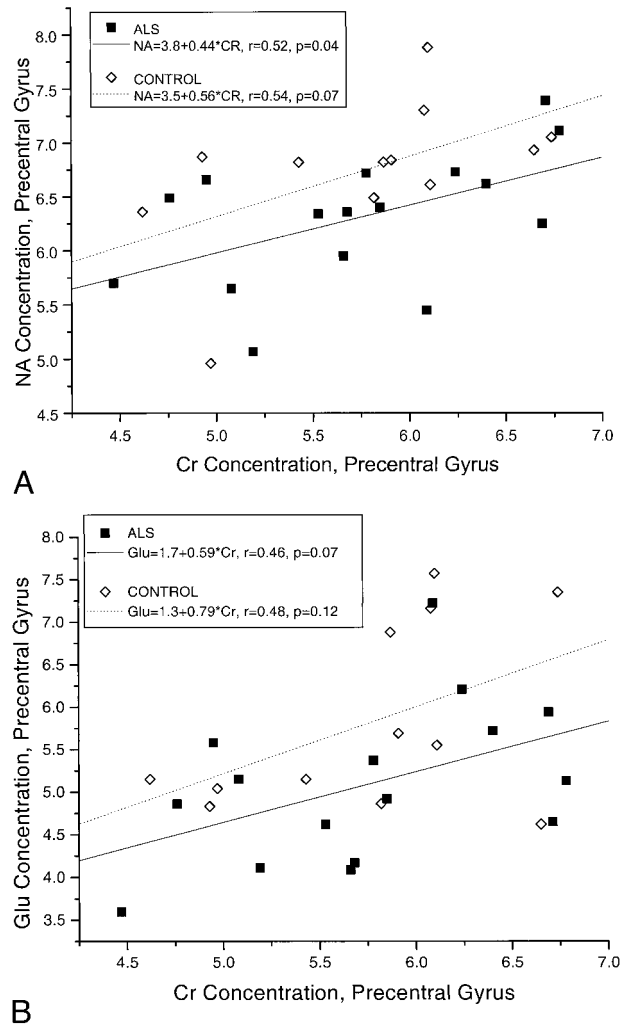‡ NS, nonsignificant; NC, no change.

FIG 3. Correlation between metabolite concentrations (mmol/L). The formulas for the regression lines are given in the *box* in the upper left-hand corner. *Asterisk* indicates multiplication; *r,* Pearson correlation coefficient for each group.
   A, NA and Cr.
   B, Glu and Cr.

observers revealed that precentral gyrus signal changes were more often reported for the FLAIR images (gray matter, nine patients; white matter, eight patients) than for the FSE images (gray matter, seven patients; white matter, two patients). For the control subjects, no signal changes were identified on the FSE images, and the agreement between observers was 100%. On the FLAIR images, however, there were signal changes in the gray and white matter of the precentral gyrus in three subjects. The two neuroradiologists agreed in their assessment of gray matter and white matter in 75% and 92%, respectively, of the control subjects.

The relationship between precentral gyrus signal changes and severity of UMN clinical findings is also presented in Table 3. For the gray matter in patients with severe clinical deficits, decreased signal intensity was observed in all cases on both FLAIR and FSE images. For the white matter in the same patients, increased signal intensity was
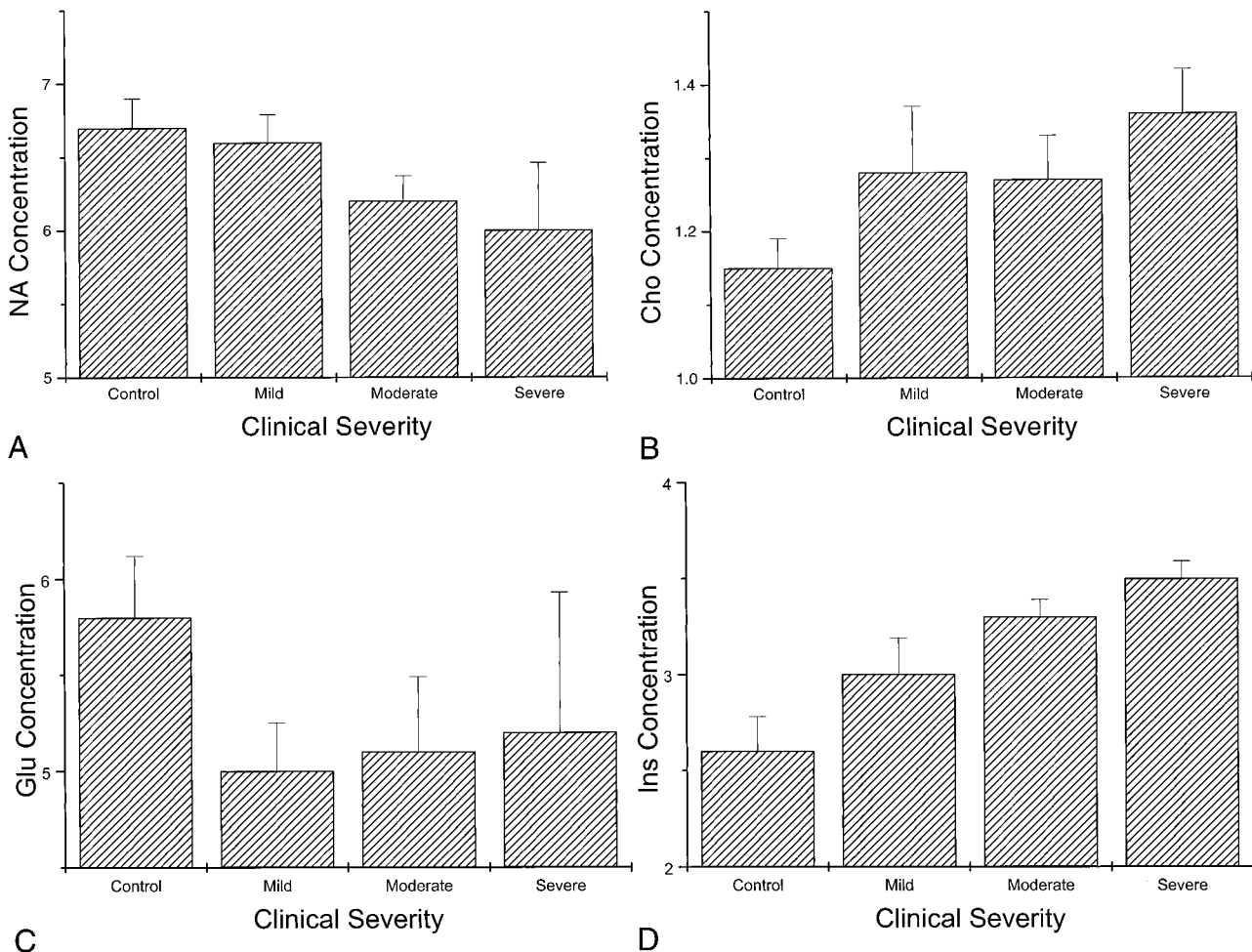
FIG 4.   Precentral gyrus metabolite concentrations (mmol/L) as a function of the severity of UMN clinical signs. The length of the *line* extending above each rectangle indicates the standard error of the mean (SEM).
A, NA.
B, Cho.
C, Glu.
D, Ins.

observed in all cases only on the FLAIR images. For the gray matter in patients with mild clinical deficits, decreased signal was detected more often on FLAIR images (three of six) than on FSE images (one of six). For the white matter in the same patients, hyperintensity was more often detected on the FLAIR images (three of six) than on the FSE images (none of six).

For each imaging sequence (FSE, FLAIR) and each region of the precentral gyrus (motor cortex gray matter, subcortical white matter), the mean metabolite concentrations of the subset of ALS patients with altered signal intensity were compared with the mean concentrations of the subset of ALS patients with isointense signal. As shown in Table 4, NA and Glu for the subset with altered signal were always lower, whereas Ins was always higher. Only the Ins difference associated with gray matter hypointensity on FSE images reached significance. The subset of seven patients with linear hypointensity in the precentral gyrus gray matter on FSE images had significantly increased ($P = .002$) Ins

(3.53 mmol/L) relative to the subset of eight patients without signal intensity changes (2.98 mmol/L).

Discussion

MR Spectroscopy

The precentral gyrus metabolite concentrations presented in Table 1 for healthy subjects are up to 30% smaller than those reported for frontal gray matter by Pouwels and Frahm (22). The primary factor responsible for these differences is probably the TR, and a secondary factor may be the method used to scale the spectra (S. Provencher, personal communication). Although technical factors may be responsible for differences between our results and those of Pouwels and Frahm (22), these factors should not affect the comparisons between ALS patients and control subjects reported in this study, since all our subjects were evaluated with the same scanner, spectral acquisition protocol, and data analysis methods.

TABLE 2: Difference in precentral gyrus metabolite concentrations (mean ± SEM, mmol/L) between first and second studies of ALS patients

Subgroup	No. of Patients	Time Interval (wk)*	NA_{diff}	Cho_{diff}	Cr_{diff}	Glu_{diff}	Gln_{diff}	Ins_{diff}
A	5	2	−0.08 ± 0.21	−0.03 ± 0.1	−0.26 ± 0.18	0.29 ± 0.87	0.02 ± 0.89	0.22 ± 0.16
B	3	11	−0.66 ± 0.1†	−0.22 ± 0.05	0.22 ± 0.72	−0.78 ± 1.03	0.07 ± 0.1	0.1 ± 0.5

*The interval between studies for each patient in subgroup A was 2 weeks; the mean interval for subgroup B was 11 weeks (range, 4–18 wk).
†The NA difference between the first (pretreatment) and second (posttreatment) studies for subgroup B was significant at P = .022. All other concentration differences for each subgroup were significant.

The overall 6% decrease in mean NA in ALS patients and the 11% decrease in the severe UMN disease subgroup relative to control subjects (Table 1) are in agreement with the results of Gredal et al (13), who reported a 9% decrease in mean NA for seven ALS patients. The in vivo spectral results are also consistent with in vitro measurements, which have shown that tissue levels of NAAG, and to a lesser extent NAA, in motor cortex are decreased (27, 28) (see following discussion of Glu results). The decrease in NA is presumably due to the neuronal degeneration and cell loss in the precentral gyrus (motor) cortex that has been demonstrated histopathologically (14). The link between motor region NA levels and UMN degeneration is further strengthened by the finding of a significant negative trend (P = .005) in NA values with increasing severity of clinical UMN signs in ALS patients (Fig 4A). This trend is consistent with the results of Rooney et al (12), who found that motor cortex NAA/(Cho + Cr) correlated with severity of UMN disease, as reflected in the maximum finger-tap rate. In our study, patients examined before and after treatment with riluzole or gabapentin, showed no clinical improvement, and in serial subgroup B there was a significant decrease in NA, suggesting ongoing neuronal loss. These results are in disagreement with the finding of Kalra et al (29) that NAA/Cr values increase toward normal levels after treatment with riluzole for 3 weeks.

The observation of decreased NA supports the conclusion that decreased NA/Cr ratio in the motor cortex of ALS patients is due to lower levels of NA (9, 10, 13). The lack of differences in NA levels between ALS patients and control subjects in the cuneus gyrus is consistent with the results of Pioro et al (9) and Ikeda et al (30). Ratio data obtained at a short TE with the STEAM method must be interpreted carefully because of the positive correlation between NA and Cr concentrations in the precentral gyrus. The correlation could be due to differences in the relative amounts of gray and white matter in the precentral gyrus voxel from patient to patient (Fig 3). Higher Cr and NA values have been found in gray matter than in white matter in some in vivo (31) and in vitro (32) MR studies. This interpretation seems unsatisfactory, since no correlation was found for the cuneus gyrus voxel. Furthermore, Cho, which is known to be significantly higher in white matter than in gray matter, showed no negative correlation with Cr in the precentral gyrus. An alternative, although unproved, interpretation is that the correlation between NA and Cr reflects a difference in neuronal energy metabolism in the two brain regions, such that Cr/phosphocreatine levels are more closely associated with neuronal integrity in the precentral gyrus (33).

The 13% increase in the precentral gyrus Cho concentration in ALS patients (Table 1) differs from the results of Gredal et al (13), who found no increase; but it is consistent with the approximately 10% increase in Cho/Cr reported by Block et al
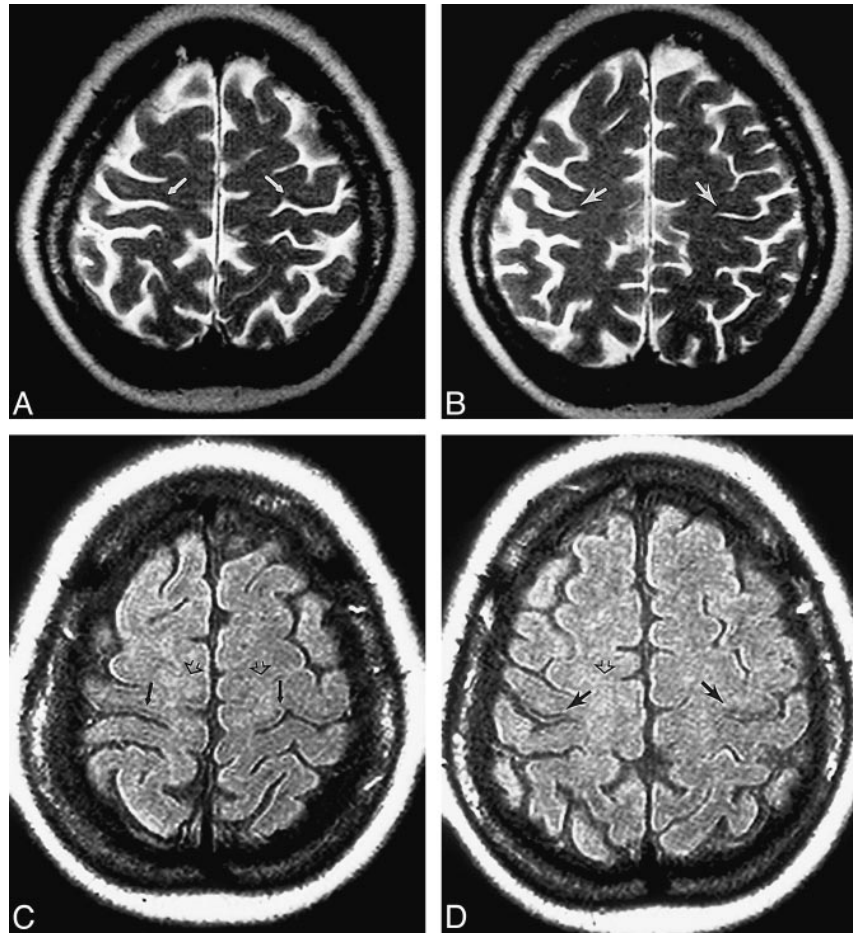
(11). Two explanations have been given for the increase in Cho signal: degradation of membrane and myelin phospholipids, as occurs in demyelinating disorders (34, 35), and glial proliferation with an increase in cell membrane precursors (11). In the precentral gyrus in ALS patients, both processes have been hypothesized, and there is histopathologic evidence of an astrocytic reaction, although it may not be limited to the motor cortex (36–38). The primary contribution to the Cho increase may be from subcortical white matter, which has roughly 30% higher Cho levels than gray matter (21, 22) and undergoes axonal degeneration and demyelination in association with motor neuron death.

Ins exhibited the largest and most significant increase in precentral gyrus concentration (Table 1), as well as the most significant trend in concentration ($P = .001$) as a function of the severity of UMN signs in ALS patients. Ins functions primarily as a brain osmolyte, yet it is also an intermediate in the metabolism of membrane-bound inositol phospholipids. It is considered a glial marker (39, 40). The elevated Ins and Cho detected in this study are compatible with changes in the phospholipid composition of myelin or other glial cell membranes or both, or in the abundance of glial cells (gliosis) in the precentral gyrus of ALS pa-

tients (40). Block et al (11) detected a 16% increase ($P < .05$) in the Ins/Cr ratio in the precentral gyrus.

There is no published study of the in vivo precentral gyrus Glu and Gln concentrations determined from short-TE spectra of ALS patients. With the LCModel method, Glu and Gln are determined separately and then added to obtain the Glx concentration. From the results in Table 1, one finds that the mean Glx value for the ALS group (8.74 mmol/L) is significantly lower ($P = .04$) than the value (10.1 mmol/L) for the control group, without adjustment for Cr covariance. Furthermore, a Glx/Cr peak area ratio, calculated from the "absolute" concentrations and corrected for the effective number of resonant protons (Glx = 5 and Cr = 3) (41), is significantly lower ($P = .045$) for the ALS group (2.55 ± 0.11) as compared with the control group (2.95 ± 0.16). Block et al (11) found that Glx/Cr peak area ratios for the ALS and control groups were not significantly different. The apparent discrepancy between our results and those of Block et al may be primarily due to differences in spectral analysis methods.

The decrease in Glx is primarily caused by the significant decrease ($P < .048$) in precentral gyrus Glu for the ALS group (Table 1). In serial studies, Glu demonstrated a large but nonsignificant de-

TABLE 3: Precentral gyrus signal intensity changes on MR images

| Group | Gray Matter | | | | White Matter | | | |
| | FSE | | FLAIR | | FSE | | FLAIR | |
	Iso	Hypo	Iso	Hypo	Iso	Hyper	Iso	Hyper
Control group	11	0	8	3	11	0	8	3
Agreement (%)*	100		75		100		92	
ALS subgroups†								
Mild	5	1	3	3	6	0	3	3
Moderate	3	2	3	2	4	1	4	1
Severe	0	4	0	4	3	1	0	4
Total								
Agreement (%)	8	7	6	9	13	2	7	8
	87		100		93		87	

Note.—FSE, fast spin-echo image; FLAIR, fast fluid-attenuated inversion recovery image; iso, isointense signal; hypo or hyper, hypointense or hyperintense signal relative to corresponding gray or white matter of middle frontal and postcentral gyri.

* Agreement refers to percentage of FSE or FLAIR images for which the two neuroradiologists reported the same signal intensity changes prior to reaching a consensus.

† The ALS group was classified into subgroups based on the severity of upper motor neuron clinical signs.

TABLE 4: Change in mean metabolite concentration and MR image signal intensity in the precentral gyrus of ALS patients

| Precentral Gyrus | Image Type | Signal | No. of Patients | Percentage of Change in Mean Concentration* | | |
				NA	Glu	Ins
Gray matter	FSE	Iso	8			
		Hypo	7	−4	−4	18†
	FLAIR	Iso	6			
		Hypo	9	−5	−11	9
White matter	FSE	Iso	13			
		Hyper	2	−11	−15	4
	FLAIR	Iso	7			
		Hyper	8	−5	−8	7

Note.—Iso, isointense signal; hypo or hyper, hypointense or hyperintense signal intensity relative to appropriate region of middle frontal and postcentral gyri.

* {[Mean concentration (subset with hypo-or hyperintense signal)/mean concentration (subset with isointense signal)] − 1} × 100%. NA and Glu have been adjusted for Cr covariance.

† Percentage of change significant at $P = .002$; all other changes are nonsignificant.

crease in those ALS patients who were followed up for a longer interval (serial subgroup B, Table 2). Furthermore, the trend in Glu concentration as a function of the severity of UMN signs approached significance ($P = .094$). The trend effect is mainly due to the higher value for the control group (Fig 4C). One interpretation of this result is that the loss of Glu occurs early in the course of the disease, preceding significant NA and neuronal loss, as has been suggested by Plaitakis (42); however, the possibility that the Glu decrease is secondary to neuronal loss cannot be excluded. The trends for Gln and Glx were clearly nonsignificant.

There is considerable evidence that altered Glu metabolism plays an important role in the pathogenesis of ALS (16, 17). Generally, with classic ALS, Glu levels are elevated in CSF (27, 42, 43) and diminished in postmortem CNS tissue (28, 44, 45). The measured CSF elevations in patients, and the extracellular Glu levels in normal brain tissue, are in the μmol/L range. While micromolar increases in extracellular, "neurotransmitter" Glu may account for excitotoxic neurodegeneration (16), these changes in concentration are not large enough to be detectable with the single-voxel proton spectroscopy methods used in this study. The intracellular Glu level in brain tissue is normally on the order of 10 mmol/L (46). This "metabolic" Glu is decreased by 30% to 45% in the spinal cord, motor cortex, and some pathologically unaffected brain regions in ALS patients (28, 44), and is apparently selective for gray matter. This change should be detectable spectroscopically, and would account for the decrease in precentral gyrus Glu observed in this study.

Our spectral data do not provide direct evidence of the hypothesized pathogenetic mechanisms, Glu excitotoxicity and defective mitochondrial energy metabolism, responsible for selective motor neuron degeneration. In a recent laboratory study, the oral administration of Cr produced a dose-dependent improvement in motor performance in transgenic ALS mice and protected them from loss of motor neurons (33). It is interesting that positive correlations between NA and Cr and between Glu and Cr were observed in the precentral gyrus but not in the cuneus gyrus of both ALS patients and control subjects. From these correlations one may speculate that neuronal metabolism of Glu and NA in the precentral gyrus is closely linked to the presence of Cr, which is involved in mitochondrial energy production and storage.

MR Imaging

There has been no attempt to correlate the finding of motor cortex hypointensity to clinical sever-

ity of UMN disease. In this study, decreased signal intensity was observed in the motor cortex of the precentral gyrus and not in nearby cortical regions on T2-weighted FSE images in 47% (7/15) of ALS patients, similar to the results of Waragai (7). The finding was detected with greater frequency on FLAIR images (60%), because of increased conspicuity in patients with mild clinical disease. In general, the frequency of detection of hypointensity varies positively with the severity of clinical UMN signs, being observed in less than 50% of patients with mild or moderate disease and in 100% of patients with severe disease, using either technique (Table 3). Cortical hypointensity was also detected on FLAIR images in 38% (3/8) of control subjects, although there was less agreement between observers with respect to the finding for control subjects than for ALS patients. These results are consistent with the known increased sensitivity of FLAIR images relative to FSE images for cortical signal changes (8) and the frequency with which hypointense signal has been previously observed in the motor cortex of healthy subjects (4, 7). In summary, hypointensity is related to motor neuron degeneration in ALS; however, it is not specific to ALS.

Published reports on the frequency and appearance of hyperintense signal in the CST of ALS patients on proton density– and T2-weighted spin-echo images have focused on the internal capsule, cerebral peduncles, and corona radiata, with occasional reference to the subcortical white matter of the precentral gyri (5, 6). As with gray matter signal changes, the FLAIR images provided increased detection of precentral, subcortical white matter hyperintensities in patients with ALS, yet also in control subjects (Table 3). The difference in detection rate for subcortical hyperintensities between the FSE (two ALS patients) and FLAIR (eight ALS patients) images was more pronounced than for cortical signal changes, especially in the severe disease clinical subgroup. For this subgroup, only FLAIR images showed signal changes in both the gray and white matter regions of the precentral gyrus in all patients with severe disease. Because of this greater conspicuity of signal changes on FLAIR images, this sequence should be included in all imaging studies of patients with clinically suspected ALS.

There have been no published data on the relationship between MR imaging findings and metabolite concentrations in the precentral gyrus region determined by localized in vivo proton spectroscopy. The comparisons in Table 4 indicate that ALS patients with signal changes on MR images tend to have greater changes in metabolite concentrations. Although the changes in NA, Glu, and Ins (Table 4), and in Cho (not shown) are statistically nonsignificant in general, they are all in the direction of a worsening metabolic state whether the signal changes are observed on FSE or FLAIR images. This suggests that with a larger number of patients, significant differences in the levels of metabolites for the two subsets of patients may become manifest. For one comparison, a significant difference was observed. ALS patients who had a hypointense band in the motor cortex on FSE images had a significantly greater Ins concentration relative to the patients without this imaging finding. Since the presence of hypointensity is not specific to ALS, it is likely that the elevated Ins concentration represents a nonspecific metabolic response to neurodegeneration. For example, motor cortex hypointensity has been observed in patients with Alzheimer's disease (47) and increased Ins/Cr ratio has been reported for various cortical locations (48). If Ins is considered a glial marker (40), then the increased Ins, without a significant change in Cho, suggests that the hypointense signal results from an astroglial response to neurodegeneration. If the glia contain excessive iron, or possibly paramagnetic species that shorten the T2 relaxation time of water protons, decreased signal would result. A similar conclusion was reached by Oba et al (4), who found astrocytes and macrophages that stained intensely with Perls stain for iron in the precentral cortex of postmortem brain specimens from patients with ALS. The iron-containing cells were sparsely distributed, however, and were only observed in three of the eight postmortem brains examined. It is more likely that paramagnetic species, such as oxygen free radicals, are responsible, particularly in view of current hypotheses about mitochondrial dysfunction associated with ALS. Conclusions that invoke the presence of iron or paramagnetic species with local susceptibility effects may be tested by acquiring gradient-echo images. Cortical signal loss on these images should be greater than that on images obtained with the FSE pulse sequence (Fig 5).

Given the possibility of a localized increase in paramagnetic species, one may question whether the differences in spectral results between ALS patients and control subjects (Table 1) are due to T2 shortening effects rather than to changes in the concentrations of metabolites. T2 effects are probably not responsible for the differences, since short TE spectra were obtained in this study and since Block et al (11) have shown that the T2 relaxation times for several metabolites (specifically Cho, Cr, and NA) in the precentral region of patients with ALS are unchanged from those of control subjects.

Conclusion

By comparing the localized proton spectra from ALS patients and control subjects, we confirmed the findings of a previous report (13) of decreased NA and made new observations regarding significantly increased Cho and Ins, and decreased Glu, in the precentral gyrus (motor cortex). Trend analyses of the metabolite concentrations as a function of the severity of clinical UMN signs provide evidence that the spectral changes reflect UMN de-

generation. Decreased Glu is consistent with in vitro evidence of the loss of intracellular metabolic Glu without specifying a mechanism. Discovery of a correlation between NA and Cr and between Glu and Cr is important from the standpoint of reporting spectral results and may support hypotheses regarding the role of mitochondrial energy metabolism in ALS (33).

MR imaging of patients with suspected ALS should include FLAIR sequences, which are more sensitive but less specific than FSE sequences for detecting signal changes in the precentral gyrus. Statistical relationships between the imaging and spectral results indicate that patients with signal changes tend to have greater decreases in NA and Glu, and greater increases in Cho and Ins. Only the relationship between motor cortex hypointensity on FSE images and elevated Ins reached significance, suggesting that a prominent astroglial response may accompany UMN degeneration. Because of the relatively small ALS clinical and imaging subgroup populations, though, most correlations between imaging findings and metabolite levels were not significant enough to establish a predictive model for the diagnosis of ALS. The inability of the combined imaging and spectroscopy results from the precentral gyrus to provide a specific diagnosis of ALS, especially in the early stages of disease, represents a drawback of this study. This may be overcome in future studies by incorporating spectral results from other CNS regions, such as the brain stem (23, 49), and the results of alternative imaging techniques (eg, diffusion tensor imaging) into a more comprehensive predictive model.

References

1. Nelson LM. **Epidemiology of ALS.** *Clin Neurosci* 1996;3:327–331
2. Leigh PN. **Pathogenic mechanisms in amyotrophic lateral sclerosis and other motor neuron disorders.** In: Calne DB, ed. *Neurodegenerative Diseases.* Philadelphia: Saunders; 1993:473–488
3. Brooks BR, Antel J, Bradley WG. **El Escorial World Federation of Neurology Criteria for the diagnosis of amyotrophic lateral sclerosis.** *Neurol Sci* 1994;124:96–107
4. Oba H, Araki T, Ohtomo K, et al. **Amyotrophic lateral sclerosis: T2 shortening in motor cortex at MR imaging.** *Radiology* 1993;189:843–846
5. Cheung G, Gawel MJ, Cooper PW, et al. **Amyotrophic lateral sclerosis: correlation of clinical and MR imaging findings.** *Radiology* 1995;194:263–270
6. Hofman E, Ochs G, Pelzl A, Warmuth-Methz M. **The corticospinal tract in amyotrophic lateral sclerosis: an MRI study.** *Neuroradiology* 1998;40:71–75
7. Waragai M. **MRI and clinical features in amyotrophic lateral sclerosis.** *Neuroradiology* 1997;39:847–851
8. Hajnal JV, Bryant DJ, Kasuboski L, et al. **Use of fluid attenuated inversion recovery (FLAIR) pulse sequences in MRI of the brain.** *J Comput Assist Tomogr* 1992;16:841–844
9. Pioro EP, Antel JP, Cashman NR, Arnold DL. **Detection of cortical neuron loss in motor neuron disease by proton magnetic resonance spectroscopic imaging in vivo.** *Neurology* 1994;44:1933–1938
10. Jones AP, Gunawardena WJ, Coutinho CM, et al. **Preliminary results of proton magnetic resonance spectroscopy in motor neurone disease (amyotrophic lateral sclerosis).** *J Neurol Sci* 1995;129 Suppl:85–89
11. Block W, Karitzky J, Traber F, et al. **Proton magnetic resonance spectroscopy of the primary motor cortex in patients with motor neuron disease: subgroup analysis and follow-up measurements.** *Arch Neurol* 1998;55:931–366
12. Rooney WD, Miller RG, Gelinas D, et al. **Decreased N-acetylaspartate in motor cortex and corticospinal tract in ALS.** *Neurology* 1998;50:1800–1805
13. Gredal O, Rosenbaum S, Topp S, et al. **Quantification of brain metabolites in amyotrophic lateral sclerosis by localized proton magnetic resonance spectroscopy.** *Neurology* 1997;48:878–881
14. Hammer RP Jr, Tomiyasu U, Scheibel AB. **Degeneration of the human Betz cell due to amyotrophic lateral sclerosis.** *Exp Neurol* 1979;63:336–346
15. Lipton SA, Rosenberg PA. **Excitatory amino acids as a final common pathway for neurologic pathway for neurologic disorders.** *N Engl J Med* 1994;330:613–622
16. Rothstein JD. **Excitotoxicity and neurodegeneration in amyotrophic lateral sclerosis.** *Clin Neurosci* 1996;3:348–359
17. Mitsumoto H, Chad DA, Pioro EP. **Excitotoxicity and oxidative damage in ALS pathogenesis.** In: *Amyotrophic Lateral Sclerosis.* Philadelphia: Davis;1998:197–225
18. Haselgrove JC, Subramanian VH, Christen R, Leigh JS. **Analysis of in-vivo NMR spectra.** *Rev Magn Reson Med* 1987;2:167–222
19. Bowen BC, Block RE, Sanchez-Ramos J, et al. **Proton MR spectroscopy of the brain in 14 patients with Parkinson disease.** *AJNR Am J Neuroradiol* 1995;16:61–68
20. Provencher SW. **Estimation of metabolite concentrations from localized in vivo proton NMR spectra.** *Magn Reson Med* 1993;30:672–679
21. Michaelis T, Merboldt K-D, Bruhn H, et al. **Absolute concentrations of metabolites in the adult human brain in vivo: quantification of localized proton MR spectra.** *Radiology* 1993;187:219–227
22. Pouwels PJW, Frahm J. **Regional metabolite concentrations in human brain as determined by quantitative localized proton MRS.** *Magn Reson Med* 1998;39:53–60
23. Pioro EP. **MR spectroscopy in amyotrophic lateral sclerosis/motor neuron disease.** *J Neurol Sci* 1997;152(Suppl 1):S49–S53
24. Naidich TP, Grant JL, Altman N, et al. **The developing cerebral surface: preliminary report on the patterns of sulcal and gyral maturation—anatomy, ultrasound and magnetic resonance imaging.** *Neuroimaging Clin N Am* 1994;4:201–240
25. Klose U. **In vivo proton spectroscopy in the presence of eddy currents.** *Magn Reson Med* 1990;14:26–30
26. Miller BL. **A review of chemical issues in 1H NMR spectroscopy: N-acetyl->/SCAP<L-aspartate, creatine and choline.** *NMR Biomed* 1991;4:47–52
27. Rothstein JD, Tsai G, Kuncl RW, et al. **Abnormal excitatory amino acid metabolism in amyotrophic lateral sclerosis.** *Ann Neurol* 1990;28:18–25
28. Tsai G, Stauch-Slusher B, Sim L, et al. **Reductions in acidic amino acids and N-acetylaspartylglutamate in amyotrophic lateral sclerosis CNS.** *Brain Res* 1991;556:151–156
29. Kalra S, Cashman NR, Genge A, Arnold DL. **Recovery of N-acetylaspartate in corticomotor neurons of patients with ALS after riluzole therapy.** *Neuroreport* 1998;9:1757–1761
30. Ikeda K, Iwasaki Y, Kinoshita M, et al. **Quantification of brain metabolites in ALS by localized proton magnetic spectroscopy (letter).** *Neurology* 1998;50:576–577
31. Doyle TJ, Bedell BJ, Narayana PA. **Relative concentrations of proton MR visible neurochemicals in gray and white matter in human brain.** *Magn Reson Med* 1995;33:755–759
32. Petroff OA, Spencer DD, Alger JR, Prichard JW. **High-field proton magnetic resonance spectroscopy of human cerebrum obtained during surgery for epilepsy.** *Neurology* 1989;39:1197–1202
33. Klivenyi P, Ferrante RJ, Matthews RT, et al. **Neuroprotective effects of creatine in a transgenic animal model of amyotrophic lateral sclerosis.** *Nat Med* 1999;5:347–350
34. Roser W, Hagberg G, Mader I, et al. **Proton MRS of gadolinium-enhancing MS plaques and metabolic changes in normal-appearing white matter.** *Magn Reson Med* 1995;33:811–817

35. Chang L, Miller BL, McBride D, et al. **Brain lesions in patients with AIDS: H-1 MR spectroscopy.** *Radiology* 1995;197:525–531

36. Dal Canto MC. **Comparison of pathological alterations in ALS and a murine transgenic model: pathogenetic implications.** *Clin Neurosci* 1996;3:332–337

37. Nagy D, Kato T, Kushner PD. **Reactive astrocytes are widespread in the cortical gray matter of amyotrophic lateral sclerosis.** *J Neurosci Res* 1994;38:336–347

38. Kushner PD, Stephenson DT, Wright S. **Reactive astrogliosis is widespread in the subcortical white matter of amyotrophic lateral sclerosis brain.** *J Neuropathol Exp Neurol* 1991;50:263–277

39. Brand A, Richter-Landsberg C, Leibfritz D. **Multinuclear NMR studies on the energy metabolism of glial and neuronal cells.** *Dev Neurosci* 1993;15:289–298

40. Frahm J, Hanefeld F. **Localized proton magnetic resonance spectroscopy of cerebral metabolites.** *Neuropediatrics* 1996;27:64–69

41. Michaelis T, Merboldt K-D, Hanicke W, et al. **On the identification of cerebral metabolites in localized 1H NMR spectra of human brain in vivo.** *NMR Biomed* 1991;4:90–98

42. Plaitakis A. **Glutamate dysfunction and selective motor neuron degeneration in amyotrophic lateral sclerosis: a hypothesis.** *Ann Neurol* 1990;28:3–8

43. Rothstein JD, Kuncl R, Chaudhry V. **Excitatory amino acids in amyotrophic lateral sclerosis: an update.** *Ann Neurol* 1991;30:224–225

44. Perry TL, Hansen S, Jones K. **Brain glutamate deficiency in amyotrophic lateral sclerosis.** *Neurology* 1987;37:1845–1848

45. Plaitakis A, Constantakakis E. **Altered metabolism of excitatory amino acids, N-acetyl-aspartate and N-acetyl-aspartyl-glutamate in amyotrophic lateral sclerosis.** *Brain Res Bull* 1993;30:381–386

46. Kvamme E, Schousboe A, Hertz L, et al. **Developmental change of endogenous glutamate and gamma-glutamyl transferase in cultured cerebral cortical interneurons and cerebellar granule cells, and in mouse cerebral cortex and cerebellum in vivo.** *Neurochem Res* 1985;10:993–1008

47. Drayer BP. **Imaging of the aging brain: II, pathologic conditions.** *Radiology* 1988;166:797–806

48. Ernst T, Chang L, Melchor R, Mehringer CM. **Frontotemporal dementia and early Alzheimer disease: differentiation with frontal lobe H-1 MR spectroscopy.** *Radiology* 1997;203:829–836

49. Cwik VA, Hanstock CC, Allen PS, Martin WR. **Estimation of brainstem neuronal loss in amyotrophic lateral sclerosis with in vivo proton magnetic resonance spectroscopy.** *Neurology* 1998;50:72–77

Appendix

ALS	Amyotrophic lateral sclerosis
ANCOVA	Analysis of covariance
ANOVA	Analysis of variance
Cho	Choline
Cr	Total creatine
CSF	Cerebrospinal fluid
CST	Corticospinal tract
FLAIR	Fluid-attenuated inversion recovery
FSE	Fast spin-echo
Gln	Glutamine
Glu	Glutamate
Glx	Glu + Gln
GPC	Glycerophosphorylcholine
Ins	*Myo*-inositol
MND	Motor neuron disease
NA	*N*-acetyl (NAA + NAAG)
NAA	*N*-acetyl aspartate
NAAG	*N*-acetyl aspartylglutamate
PCh	Phosphorylcholine
PRESS	Point-resolved spectroscopy
STEAM	Stimulated-echo acquisition mode
UMN	Upper motor neuron